

Unsupervised Novel View Synthesis from a Single Image

Pierluigi Zama Ramirez^{1,2}
pierluigi.zama@unibo.it

Diego Martin Arroyo²
martinarroyo@google.com

Alessio Tonioni²
alessiot@google.com

Federico Tombari^{2,3}
tombari@google.com

¹University of Bologna

²Google Inc.

³ Technische Universität München

Abstract

Novel view synthesis from a single image has recently achieved remarkable results, although the requirement of some form of 3D, pose, or multi-view supervision at training time limits the deployment in real scenarios. This work aims at relaxing these assumptions enabling training of conditional generative models for novel view synthesis in a completely unsupervised manner. We first pre-train a purely generative decoder model using a 3D-aware GAN formulation while at the same time train an encoder network to invert the mapping from latent space to images. Then, we swap encoder and decoder and train the network as a conditioned GAN with a mixture of an autoencoder-like objective and self-distillation. At test time, given a view of an object, our model first embeds the image content in a latent code and regresses its pose, then generates novel views of it by keeping the code fixed and varying the pose. We test our framework on both synthetic datasets such as ShapeNet and on unconstrained collections of natural images, where no competing methods can be trained.

1. Introduction

Novel View Synthesis (NVS) aims to generate novel viewpoints of an object or a scene given only one or few images of it. Given its general formulation, it is one of the most challenging and well-studied problems in computer vision, with several applications ranging from robotics, image editing, and animation to 3D immersive experiences.

Traditional solutions are based on multi-view reconstruction using a geometric formulation [12, 16, 54]. Given several views of an object, these methods build an explicit 3D representation (*e.g.* mesh, pointcloud, voxels...) and render novel views of it. A more challenging problem is novel view synthesis given just a single view of the object

as input. In this case, multi-view geometry cannot be leveraged, making this an intrinsically ill-posed problem. Deep learning, however, has made it approachable by relying on inductive biases, similarly to what humans do. For instance, when provided with the image of a car, we can picture how it would look from a different viewpoint. We can do it because, unconsciously, we have learnt an implicit model for the 3D structure of a car, therefore we can easily *fit* the current observation to our mental model and hallucinate a novel view of the car from a different angle. This work tries to replicate a similar behaviour using a deep generative model.

Several works have recently investigated this line of research [69, 34, 46] by designing category-specific models that, at test time, can render novel views of an object given a single input view. However, all these methods require expensive information at training time such as 3D supervision [51] or multi-view images of the same object with known camera poses [15, 74, 34, 69, 22]. Our initial research question was: *How can we learn to hallucinate novel views of a certain object from natural images only?* Finding an answer would allow deployment to any object category without being constrained to synthetic benchmarks or well-crafted and annotation-intensive datasets.

Inspiration for our work comes from the recent introduction of 3D-aware GAN models [40, 41, 32, 53], which allow to disentangle the content of a scene from the viewpoint from which it is observed. These methods can *generate* objects and synthesize views of them from a random latent vector. However, they cannot be directly used to synthesize novel views of a *real* object unless some form of inversion or conditioning is applied.

We propose a novel framework for NVS based on inverting the knowledge of a 3D-aware GAN by means of self-distillation. Our framework is composed of an encoder network that projects an input image to a latent vector and an estimated pose, and a decoder architecture that, from the estimated latent vector, recreates the input view (with the

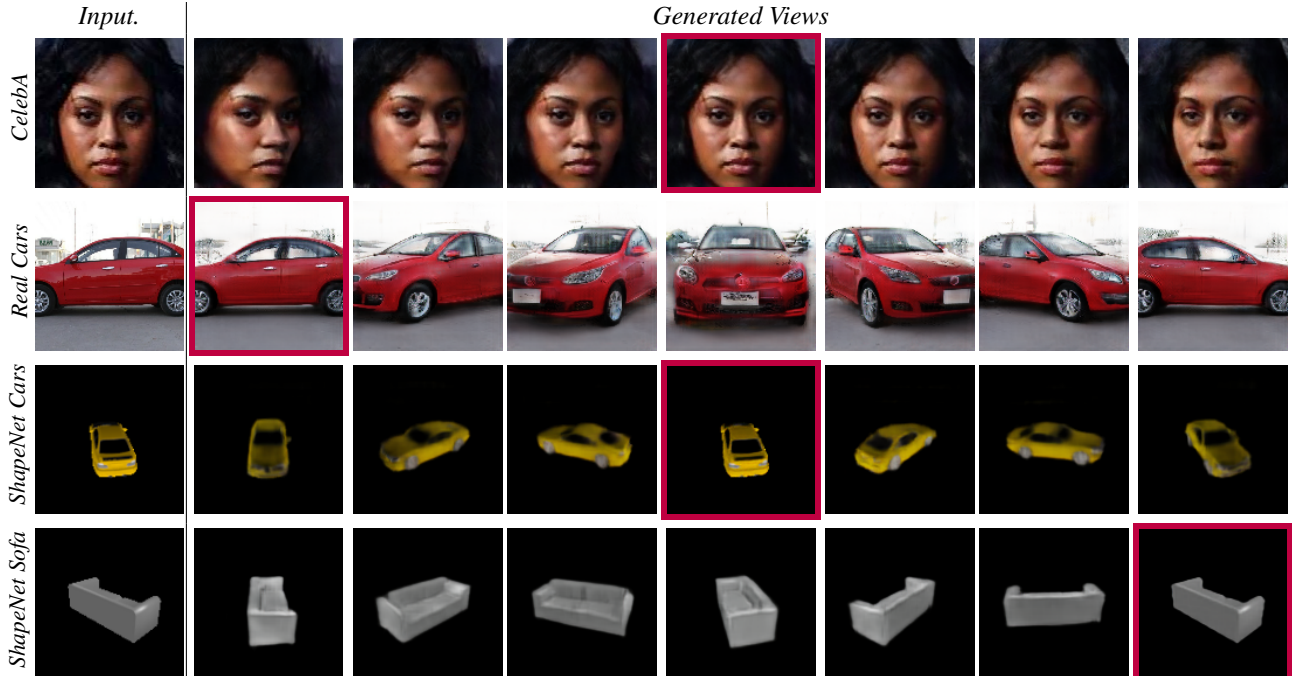


Figure 1. Novel view synthesis from a single input image. We train our method on a set of natural images of a certain category (*e.g.* faces, cars...) without any 3D, multi-view or pose supervision. Given an input image (left column) our model estimates a global latent representation of the object and its pose to reconstruct the input image (images framed in red in each row). By changing the pose we can synthesize novel views of the same object (columns 2-8).

estimated pose) or generates novel views (by changing the pose). We design a two-stage training procedure for this system. In the first stage, we train the decoder as a 3D generative model, *i.e.*, to synthesize images of new objects by sampling random latent representations. At the same time we also pre-train the encoder to invert it by estimating the latent vector and pose of a generated image. Then, in the second stage, we swap the position of encoder and decoder turning the network into a 3D autoencoder for NVS and train it to reconstruct real images. Given the change of order between encoder and decoder in the two stages of our approach we named it *Disassembled Hourglass*.

Contrary to pre-existing GAN inversion methods [76, 11] we propose to finetune the weights of the generator during this stage to achieve better reconstruction results. In order to avoid a degenerate solution that does not maintain the 3D structure of the object, we propose to self-distill the knowledge of the generative model obtained in the first step. In practice, we use it to generate multiple views for a sampled latent code, then we feed to the decoder one of the generated viewpoints and directly supervise it to reconstruct a different view of the same object. Supported by experimental results, we argue that this is key to learn a network able to achieve meaningful high quality NVS. Finally, an optional third step finetunes the network on a specific image to recover fine details with just few optimization steps.

We show in Fig. 1 qualitative results of our framework on the standard benchmark for NVS ShapeNet [8], as well as datasets of real images [35, 72], where competitors cannot be trained due to the lack of pose annotations. We will release the code in case of acceptance. To summarize our contributions:

- We introduce a novel framework for NVS to generate novel views of a given object from a single input image, while at the same time regressing the image pose.
- We propose the first framework which can be trained on natural images without any form of explicit supervision besides representing objects of a certain category.
- We introduce a two-stage training approach that allows to self-distill the knowledge of a 3D-aware generative model to make it conditioned while preserving disentanglement of pose and content.

2. Related Works

2.1. Novel View Synthesis

Traditional approaches for the NVS problem are based on multi-view geometry [12, 16, 54]. They estimate an explicit 3D representation (*e.g.*, mesh) of the object, then render novel views from it. More recently several approaches

| Method | Train | | | Test |
|----------------|-------|------|-----------|-------------|
| | 3D | Pose | Multiview | Source Pose |
| MV3D [59] | ✓ | ✓ | ✓ | ✗ |
| AF [75] | ✗ | ✓ | ✓ | ✗ |
| CORN [22] | ✗ | ✓ | ✓ | ✓ |
| SHARF [51] | ✓ | ✓ | ✓ | ✓ |
| CRGAN [60] | ✗ | ✓ | ✓ | ✗ |
| TBN [46] | ✗ | ✓ | ✓ | ✗ |
| SRN [57] | ✗ | ✓ | ✓ | ✓ |
| PixelNerf [74] | ✗ | ✓ | ✓ | ✓ |
| ENR [15] | ✗ | ✓ | ✓ | ✗ |
| VIGAN [69] | ✗ | ✓ | ✓ | ✓ |
| AUTO3D [34] | ✗ | ✗ | ✓ | ✗ |
| Ours | ✗ | ✗ | ✗ | ✗ |

Table 1. Requirements of methods for Novel View Synthesis from a single image.

based on CNNs have been proposed. Some of them, inspired by traditional 3D computer vision, train networks to explicitly estimate a 3D representation of the object such as mesh [49], point-cloud [33]), voxel map [23], depth map [18, 68] and then use it for rendering. All these methods need some kind of 3D supervision, except for [66] which however assumes quasi symmetric objects to generate a mesh from a single view. A different line of work is represented by learning-based approaches, which estimate novel views by directly mapping a source to a target view [27, 14, 75, 47, 60, 61, 58, 59, 69, 71] without explicit estimation of a 3D model. Typically these methods achieve better NVS performance thanks to their ability to hallucinate views even when no geometric information is available (e.g., parts outside of the object mesh). Among them, we find approaches suitable for a single object instance [36, 56, 38] or able to generalize to novel scenes/objects [52, 57, 9, 65, 34, 69, 22, 73, 59, 75, 46, 79, 17]. Training an instance-specific model produces higher quality results at the cost of longer training times for each object. General approaches are trained once per category and thus can be more easily deployed on real problems. However, all the proposed solutions require poses, 3D models or multiple views as training supervision. We report in Tab. 1 a list of relevant learning based methods for novel view synthesis from a single image and their requirements at training or test time. To the best of our knowledge ours is the first work to relax these assumptions and learn a category-specific network for NVS from natural images only.

2.2. Inverting Generative Models

Generative Adversarial Networks (GANs) [19] have been applied to many computer vision applications, making them the most popular generative models. Thanks to recent discoveries in terms of architecture [7, 28, 25, 48], loss functions [37, 6], and regularization [39, 21], GANs

are able to synthesize images of impressive realism [28, 7]. A recent line of work explored the possibility of inverting a pre-existing generator to use it for image manipulation tasks. These approaches propose strategies to map an image into the generator latent space, and to navigate it to produce variants of the original picture. Two main families of solutions have been proposed for this task: passing the input image through an encoder neural network [30, 76] or optimizing a random initial latent code by backpropagation to match the input image [2, 3, 11, 76]. Both techniques look for the latent variable that better reconstructs the input image while keeping the generator frozen. Recent works [2, 3, 20, 67, 70] achieve incredible inversion results by focusing on StyleGAN, which however limits their applicability when used on different architectures. More general solutions still have limitations on the reconstruction quality. Indeed, *inverting* a generative model is notoriously difficult due to the complexity and non convexity of the generator latent space [76] or due to the limited variability of objects that can be generated by it. In our work, along the lines of this research avenue, we propose a method to embed real images of a 3D-aware generative model allowing for identity-preserving transformations in pose (also known as Novel View Synthesis).

Existing GAN inversion works keep the generator frozen in order to maintain the properties of the latent space, making it more difficult to further improve the image reconstruction. However, 3D-aware GANs disentangle the pose from the latent space, enabling finetuning of the generator without losing control on the pose. We propose to use this property during the second stage of our method to finetune the generator and greatly improve the reconstruction quality.

Similar directions have been explored in ConfigNet [31] which proposes to use an encoder to embed face images into a disentangled latent space for several attributes (e.g. color, haircut, pose...) allowing a great variety of explicit image manipulations. However, the method needs a 3D synthetic parametric model to generate training data and therefore it has been tested only on faces. Our method instead does not need any form of parametric model, but can be trained on a simple collection of natural images.

2.3. 3D-Aware Neural Image Synthesis

Generative models have recently been extended with different forms of 3D representations embedded directly in the network architecture [32, 4, 40, 63, 77, 53] to synthesize objects from multiple views. The majority of methods require 3D supervision [63, 77] or 3D information as input [45, 4]. [24, 40, 53] train generative models without supervision from only a collections of natural images. [24] learns a textured 3D voxel representation from 2D images using a differentiable render, while HoloGAN [40] and some related works [32, 41, 43] learn a low-dimensional 3D feature

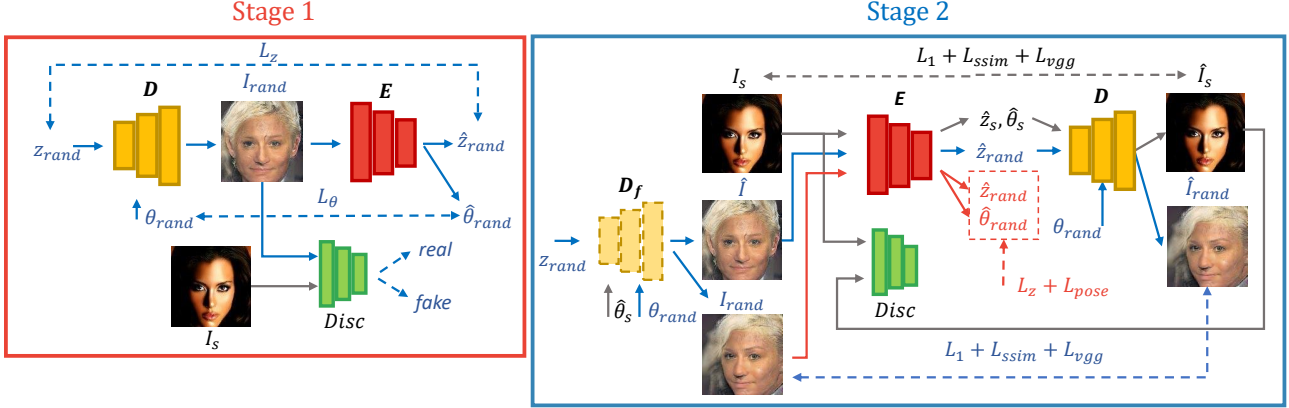


Figure 2. Overview of *Disassembled Hourglass*. During the first stage (left) we train a 3D-aware decoder (D) network using a generative formulation while simultaneously training an encoder (E) to invert the generation process and regress the latent code z and the pose θ . Then, during the second stage (right), we swap the encoder with the decoder and train the model in an autoencoder fashion to reconstruct real images and self-distill the pre-trained generative model to keep multi-view consistency.

combined with a 3D-to-2D projection. GRAF [53] leverages neural radiance fields [38] conditioned on a random variable to enable generation of novel objects. We build on these recent findings and extend 3D aware generative models to perform novel view synthesis from natural images.

3. Method

The key concept behind the proposed framework is to exploit the implicit knowledge of 3D-aware generative models in order to perform novel view synthesis. Fig. 2 shows an overview of the proposed approach.

Defined as θ_s and θ_t a source and a target unknown viewpoints, our goal is to synthesize a novel view I_t from θ_t given only a single image I_s representing an object from the view θ_s . Our framework, namely *Disassembled Hourglass*, is composed of two main components: an encoder E and a decoder D . E takes as input I_s and estimates a global latent representation z_s jointly with the source view θ_s . D , instead, is a 3D-aware generative model: given a global latent object representation z , and a target view θ , it can generate an image depicting the object in the requested view. However, differently from the generative literature, we aim to use D to generate novel views of a specific *real* object rather than a *generated* one.

3.1. Stage 1: Generative Training

A naive solution for our problem could be to train an autoencoder to reconstruct images, *i.e.* $\theta_t = \theta_s$. A similar solution was used by [46] but relying on multi-view supervision at training time. However, in our scenario we cannot enforce multi-view consistency due to the lack of annotations, therefore the network is free to learn incomplete representations that are good to reconstruct the input image but cannot be used to generate novel views, *e.g.* it might learn

to ignore the pose. We will show experimental results to support this claim in Sec. 5.3. To overcome this problem, we decide to train our framework in a generative manner in a first training step: *Stage 1*. In particular, we train D to create realistic views starting from randomly sampled latent representations, z_{rand} , and poses, θ_{rand} . This stage helps D to learn a good initial representation for the object category. Recent 3D-aware generators [40, 53] can be trained without using any kind of supervision, therefore for Stage 1 we use only natural images. We train our generative model using a standard adversarial loss L_{adv} which involves the use of a discriminator, $Disc$. Jointly with D , we also train an encoder E to map a generated image to its latent space and pose.

Overall, we use D to generate an image $I_{rand} = D(z_{rand}, \theta_{rand})$ from a randomly sampled latent code and pose; then we optimize E to invert the generation process, estimating the view $\hat{\theta}_{rand}$ and latent vector \hat{z}_{rand} by minimizing the following losses:

$$L_z = \mathbb{E} \|z_{rand} - \hat{z}_{rand}\| \quad (1)$$

$$L_\theta = \mathbb{E} \|\theta_{rand} - \hat{\theta}_{rand}\| \quad (2)$$

3.2. Stage 2: Reconstruction Autoencoder

Given a real image, we could use E to estimate a z and $pose$ that would project it into the learned generator latent space and, in turn, use D for image reconstruction and NVS (changing $pose$ while keeping z). However, this *GAN inversion* task is notoriously difficult due to the non-convexity of the generator latent space [76]. In practice very often the z and $pose$ predicted for real images generate very poor reconstructions (see Sec. 5.2). We argue that we might obtain much better results by finetuning the weights of the generator differently from standard inversion approaches. Typi-

cally, these methods keep the generator frozen to preserve the structure of the generative space and be able to perform image editing tasks in it. However, in our case the architecture of D disentangles the *pose* from z by construction, therefore even if we finetune the weights of the generator we could always retain the ability to modify the pose of the generated images. Thus, in *Stage 2*, we swap the decoder with the encoder, rebuilding the original autoencoder structure, and we train the whole system to reconstruct real images in an end-to-end fashion.

Summarizing, given a source real image I_s we propagate it through the encoder E to get the corresponding $E(I_s) = (\hat{z}_s, \hat{\theta}_s)$, i.e., the predicted latent vector and view respectively. At this point, we use D to reconstruct the original image $\hat{I}_s = D(\hat{z}_s, \hat{\theta}_s)$ by starting from the pre-trained D and E from Stage 1. We train our system with a combination of pixel wise L_2 , perceptual [26] L_{vgg} , and SSIM [64] L_{ssim} losses, defined as follows:

$$L_2 = \mathbb{E} \|I_s - \hat{I}_s\| \quad (3)$$

$$L_{vgg} = \sum_i \mathbb{E} \|V_i(I_s) - V_i(\hat{I}_s)\| \quad (4)$$

$$L_{ssim} = \mathbb{E} (1 - SSIM(I_s, \hat{I}_s)) \quad (5)$$

where V_i are features extracted at the i -th layer of a VGG16 [55] backbone pre-trained on ImageNet [13]. We experimentally achieved best reconstruction results by using the output of the *block2_conv2* layer. Moreover, to increase the quality and details of the reconstruction, we follow the example of [25] and we train the generator adversarially with *Disc* using the DCGAN [50] loss, L_{adv} , computed using I_s as real samples and \hat{I}_s as fake samples. Since our generator is pre-trained, to stabilize the adversarial learning, we start from the pre-trained *Disc* of Stage 1.

3.3. Stage 2: Distilling the Generative Knowledge

As supported by experiments in Sec. 5.3, we verified that by simply finetuning the network for reconstruction on all images, it will collapse to an inconsistent 3D representation that cannot be used to synthesize novel views by changing θ . Nevertheless, we know that D has a consistent 3D representation at the end of Stage 1. Thus, we force our network to preserve such a crucial property by *self-distilling* the knowledge from a frozen version of itself, namely D_f . To do so, we train the model on a set of images generated by D_f . For these images we can have both “labels” for their latent code and pose, as well as multiple-views of the same object. We use all these information to train the encoder and decoder with direct supervision. Thus, for the training of E , given a random latent vector z_{rand} and a random view θ_{rand} we generate an image from the frozen decoder D_f as $I_{rand} = D_f(z_{rand}, \theta_{rand})$. Then, we can predict \hat{z}_{rand} and $\hat{\theta}_{rand}$ from $E(I_{rand})$ and apply the consistency

losses described in Eq. (1) and Eq. (2). For the training of D , given z_{rand} and θ_s , we use D_f to generate a novel view of the same object, \hat{I} . Instead of applying the standard autoencoder loss, we use E and D to reconstruct a novel view of the object and provide direct supervision on it. By doing so we preserve the consistency of 3D-representations by maintaining good geometric priors. To do so, the encoder predicts the latent vector \hat{z}_{rand} from \hat{I} and the decoder generates a novel view as $\hat{I}_{rand} = D(\hat{z}_{rand}, \theta_{rand})$. Then, we apply the previous reconstruction losses to the novel view:

$$L_2^{gen} = \mathbb{E} \|\hat{I}_{rand} - I_{rand}\| \quad (6)$$

$$L_{vgg}^{gen} = \sum_i \mathbb{E} \|V_i(\hat{I}_{rand}) - V_i(I_{rand})\| \quad (7)$$

$$L_{ssim}^{gen} = \mathbb{E} (1 - SSIM(\hat{I}_{rand}, I_{rand})) \quad (8)$$

At test time given an input image I of an object we can use E to predict the corresponding (z, θ) , by keeping z fixed and changing θ we can easily synthesize novel views of the specific object depicted in I .

3.4. Self-Adaptation by finetuning

Finally, we propose an optional final step where we employ one-shot learning to finetune our network on a specific target image with a self-supervised protocol. We use the set of losses L_2 , L_{ssim} , L_{vgg} , and L_{adv} to optimize the parameters of D and the value of (z, θ) by back-propagation starting from the initial values provided by E . This step is optional but we will show in Sec. 5.2 how it can improve quality by adding some fine details to the reconstructed images without downgrading the ability to generate novel views.

4. Experimental Settings

4.1. Network Architectures.

We focus on experiments using HoloGAN [40] as D , because of its lower computational requirements w.r.t. neural radiance field generators [53]. The lightweight architecture of HoloGAN allows us to employ image-wide perceptual losses which are extremely important to achieve better performance (see Sec. 5.5). For neural radiance fields models the generation of a full frame for each training sample would prohibitively increase the computational costs. However, we do recognize the interesting properties of NeRF-based methods and for this reason we report preliminary results using GRAF as generator in Sec. 5.6. We modify the basic architecture of HoloGAN by using for up-sampling 3x3 convolutions followed by a bilinear sampling instead of deconvolutions to decrease the well known grid artifacts problem [44]. HoloGAN encodes the pose θ as the azimuth and elevation of the object with respect to a canonical reference system which is learnt directly from the network, assuming the object being at the center of the scene.

| Name | Type | # Training/Val/Test | Resolution | Azimuth | Elevation | Scaling |
|-------------------|-----------|------------------------|------------|-----------|-----------|---------|
| CelebA [35] | Real | 162770 / 19867 / 19962 | 128x128 | 220°-320° | 70°-110° | 1.0 |
| Real Cars [72] | Real | 95410 / 13633 / 27267 | 128x128 | 0°-360° | 60°-95° | 1.0-1.5 |
| Shapenet-Cars [8] | Synthetic | 125928 / 18000 / 35976 | 128x128 | 0°-360° | 25°-30° | 1.0-1.5 |
| Shapenet-Sofa [8] | Synthetic | 53304 / 7608 / 15239 | 128x128 | 0°-360° | 25°-30° | 1.0-1.5 |

Table 2. Additional Datasets Information

Moreover, it uses a scale parameter representing the object dimension which is inversely related to the distance between the object and the virtual camera. We use the same parametrization and train E to estimate θ as azimuth, elevation, and scale. E is composed of three stride-2 residual blocks with reflection padding followed by two heads for pose and z regression. The pose head is composed of a sequence of 3x3 convolution, average pooling, fully connected and sigmoid layers. The estimated pose is remapped from $[0,1]$ into a given range depending on the datasets. The z head has a similar architecture except for the tanh activation at the end. z is a 1D array of shape 128 except for Real Cars when we use shape 200. During Stage 1 we sample z from a $[0, 1]$ uniform distribution.

4.2. Training Details.

Our pipeline is implemented using Tensorflow [1] and trained on a NVIDIA 1080 Ti with 11 GB of memory. During Stage 1 we use a procedure similar to the one described in [40]. We train our networks for 50 and 30 epochs for Stage 1 and 2 respectively. We use Adam [29] with β_1 0.5 and β_2 0.999. Initial learning rate is $5 * 10^{-5}$ and after 25 epochs we start to linearly decay it. During the optional third stage we finetune for 100 steps with learning rate 10^{-4} .

4.3. Datasets.

We evaluate our framework on ShapeNet [8], CelebA [35] and Real Cars [72]. We train at resolution 128x128 for all datasets. Even when available, we did not make use of any annotations during training. ShapeNet [8] is a synthetic dataset of 3D models belonging to various categories. We tested our method in the *cars* and *sofa* categories using renderings from [10] as done in [69, 34]. For each category, following the standard splits defined in [69, 34], we use 70% of the models for training, 20% for testing and 10% to validate our approach. Even though the dataset provides multiple views of each object, we did not use this information at training time since our method does not require any multi-view assumption. CelebA [35] is a dataset composed of 202599 images of celebrity faces. We use the aligned version of the dataset, center cropping the images. Real Cars [72] is a large scale dataset of real cars composed of 136726 images. For real datasets we split them in 80% for training and 20% for testing. We make use of the bounding box provided from the dataset to crop out a square with the same

| | Train | | | Test | Sofa | |
|--------|-------|------|-----------|-------------|------------------|-----------------|
| Method | 3D | Pose | Multiview | Source Pose | $L_1 \downarrow$ | SSIM \uparrow |
| [59] | ✓ | ✓ | ✓ | ✗ | 17.52 | 0.73 |
| [75] | ✗ | ✓ | ✓ | ✗ | 13.26 | 0.77 |
| [69] | ✗ | ✓ | ✓ | ✓ | 10.13 | 0.83 |
| [34] | ✗ | ✗ | ✓ | ✗ | 10.30 | 0.82 |
| Ours | ✗ | ✗ | ✗ | ✗ | 13.83 | 0.72 |

Table 3. Evaluation of NVS using a single input image on the ShapeNet-Sofa dataset. The best results are highlighted in bold. When computing the L_1 error, pixel values are in range of $[0, 255]$.

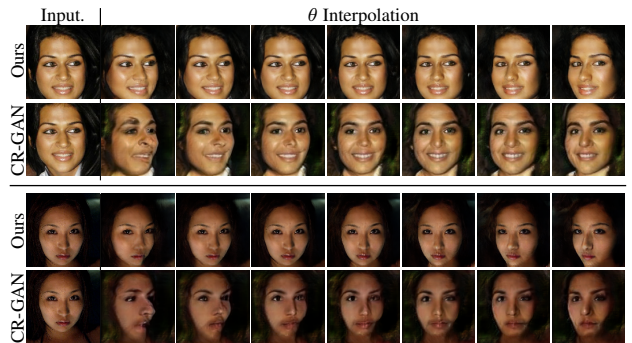


Figure 3. Qualitative comparison vs CR-GAN [60] on CelebA. For each input, top row is our method, bottom row is CR-GAN.

center and size equal to the largest side of the car bounding box. If the square exceeds image dimensions, we crop the largest possible square. Then, we resize images at 128x128.

Finally, in Tab. 2 we report additional information on our training datasets.

5. Experimental Results

5.1. Novel View Synthesis

Quantitative Comparison. We investigate the performance of our Stage 2 (no image-specific finetuning) framework for NVS from object rotation. We compare mainly against Auto3D [34] because it is the work with the requirements closer to ours (even if requires multi-view images at training time while we don't). We follow the protocol defined by Auto3D and we show the performance of single image NVS for the class Sofa in ShapeNet [8]. We do not report results for the classes Bench and Chairs because our generative model based on HoloGAN during stage 1 failed to find a meaningful 3D representation for those classes (more on this in Sec. 6). For each pair of views of an object, (I_s, I_t) , we evaluate the L1 (lower is better) and SSIM

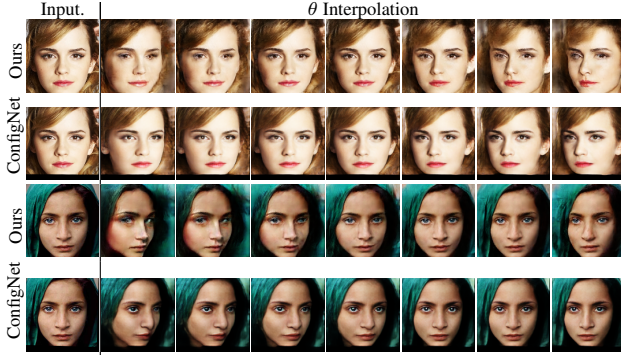


Figure 4. Qualitative comparison against ConfigNet [31] on downloaded web images. For each input image, the top row is our method, while the bottom row is ConfigNet.

[64] (higher is better) reconstruction metrics and we report results in Tab. 3. Given an input image I_s , we first estimate the global latent vector $z_s = E(I_s)$. Then, we generate the target view $I_t = D(z_s, \theta_t)$ using the ground-truth target pose θ_t . When computing the L_1 error we use pixel values in range $[0, 255]$. Since the pose estimated by our network is aligned to a learnt reference system which may differ from the one of ShapeNet, we train a linear regressor on the training set to map the ground-truth reference system into the learnt one. We use this mapping at test time to compare our method with other works. However, this is not needed in practise, and it could be a source of error during the evaluation. Our method achieves results comparable to MV3D [59] with a lower L1 error but with a slightly lower SSIM. Compared to the other works we achieve slightly worse performance, however, as highlighted in Tab. 1, all competitors require multiple views of the same object or ground-truth poses [59, 75, 69], while we do not.

Qualitative Results. In Fig. 3 we extend the test to a real dataset and qualitatively compare against CR-GAN [60] on the test set of CelebA. For CR-GAN we use the original code implementation and pre-trained weights available online and we pre-process images as described in the paper, which is different from our pre-processing, leading to slightly different inputs. Our method consistently achieves better results since it better preserves the identity of the input image and the 3D structure, especially for the extreme views from the side. We wish to highlight that CR-GAN was pre-trained with multi-view and pose supervision on the 300wLP dataset [78] before being fine tuned on CelebA. Moreover CR-GAN addresses pose estimation as a classification task, therefore it can generate only a fixed number of poses, while our method allows to sample continuous poses.

In Fig. 4, we compare our results against ConfigNet [31] on random portrait images downloaded from the web. For ConfigNet we align the faces using the pre-processing based on OpenFace [5] as in the original paper, thus the inputs are slightly different (e.g. thin black borders for ConfigNet).

| Method | L1 | SSIM | PSNR |
|--------------------|-------|------|-------|
| [11] | 65.79 | 0.25 | 10.07 |
| [76] | 31.18 | 0.40 | 15.43 |
| Stage 2 | 23.83 | 0.50 | 18.01 |
| Stage 2 + Finetune | 5.23 | 0.90 | 31.00 |

Table 4. Reconstruction quality on CelebA of various inversion strategies. For L1 error, pixel values are between $[0, 255]$.

We used the original code implementation available online and the pre-trained weights on FFHQ [28]. We notice that our network achieves comparable results, slightly better for poses closer to the input image, while worse for far poses. However, differently from our method, ConfigNet requires large synthetic datasets with labels for pose and several semantic attributes for an initial supervised training, while we do not have this type of constraint. We argue that while it is remarkable that high quality rendering of faces can be used to pre-train a model with supervision, it is hard to think of extending the same procedure to any other object categories we might be interested in, since it requires curated 3D modeling and expensive rendering times. Our model provides comparable performance without these requirements since we only need a collection of natural images.

Finally, in Fig. 5 we show additional qualitative results of our method after finetuning for CelebA [35], Real Cars [72], Shapenet-Cars [8] and Shapenet-Sofa [8].

5.2. Comparison with GAN inversion

We now want to explore the fidelity that our framework can achieve when inverting the generative model D . In Tab. 4 we compare reconstruction results on 2000 random samples of the test set of CelebA of our Stage 2 and Stage 2 with image specific finetuning against inversion methods directly applied on D at the end of stage 1. In particular we consider *fitting* the latent space of a generative model as done in [11] or using an encoder trained to invert a frozen generator, to initialize z as done in [76]. We focus on these two inversion methods since they are general purpose and not explicitly designed around one generator architecture, e.g., [2, 3] for StyleGAN. In Fig. 6, we show a qualitative comparison of these approaches. Our Stage 2 (row 3) technique can already achieve much better performance w.r.t. the other two methods (rows 1 and 2), which demonstrates that by finetuning the weights of the generator the network achieves much higher reconstruction fidelity. Moreover, the finetuning (row 4) on a single test image dramatically improve the results, achieving impressive image reconstructions. We notice that our method recovers fine details such as hair, eyes and skin color, and can still rotate objects meaningfully. We also tried to alternate the fitting of z and pose to avoid ambiguities in the optimization process, achieving comparable results. These results support

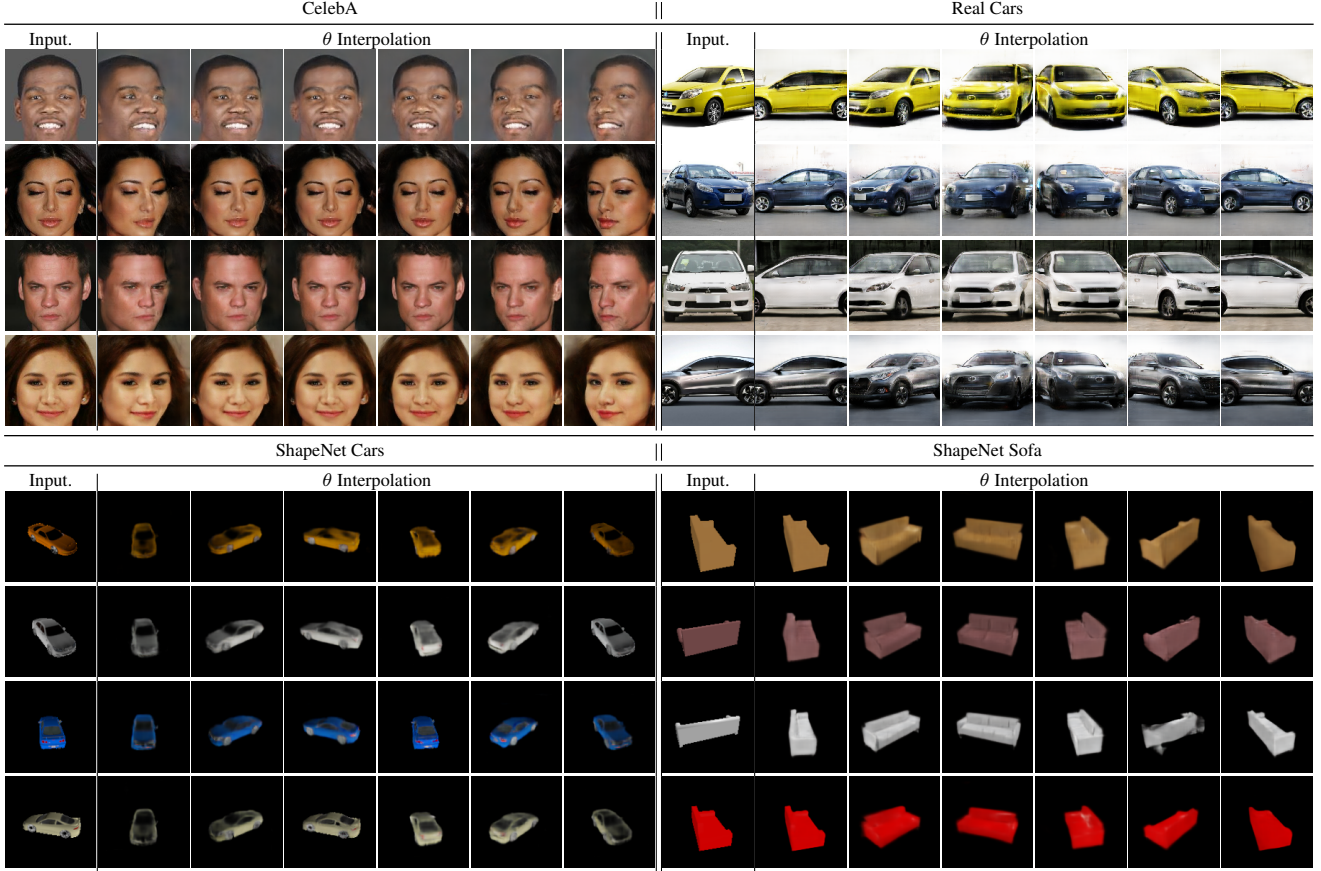


Figure 5. Qualitative results on CelebA [35], Real Cars [72], ShapeNet-Cars [8], ShapeNet-Sofa [8].

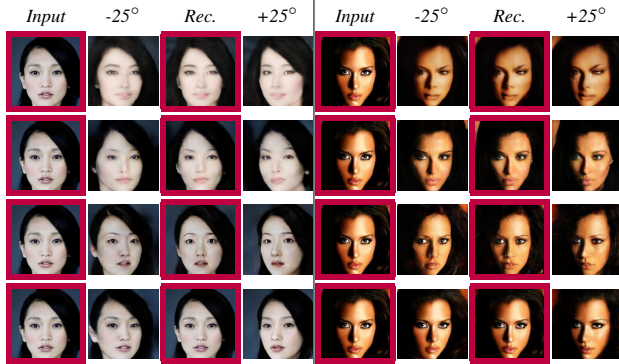


Figure 6. Qualitative comparison between different inversion strategies. From top to bottom: [11], [76], our Stage 2, our Stage 2 + image-specific finetuning. From left to right: input, azimuth rotations respect to the input of -25° , 0° (reconstruction), and 25° .

our intuition that by finetuning the weights of the generator (last two rows) we achieve much better reconstructions.

In Fig. 7, to further evaluate the effectiveness of our finetuning we plot the L_1 reconstruction error of our finetuning method (left plot) and [11] (right plot) during training on 25 randomly sampled test images (an image per plotted line). Images are always normalized in the range $[-1, 1]$ during

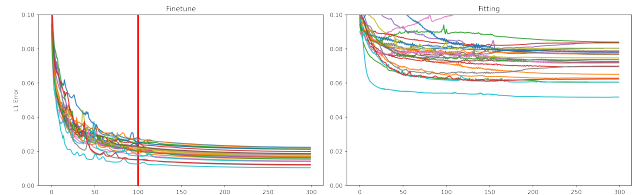


Figure 7. L_1 training reconstruction error of 25 test samples from CelebA. Left plot: *Finetuning* (Ours), the red line denotes the iteration we used for early stopping in our experiments. Right plot: *Fitting* with [11]. Same samples have the same color in the two plots. Pixel intensities in the images are normalized in the range $[-1, 1]$.

training. The left plot shows that our method converges to a much lower error (approximately a third of the *fitting* one) and in a more stable way across test samples. Indeed, after only 100 optimization steps (vertical red line in left plot) we are able to perform early stopping since our method has already converged to a stable solution for almost all samples. The right plot instead shows how for the *fitting* strategy we had to train for approximately 300 steps before reaching stable solutions.

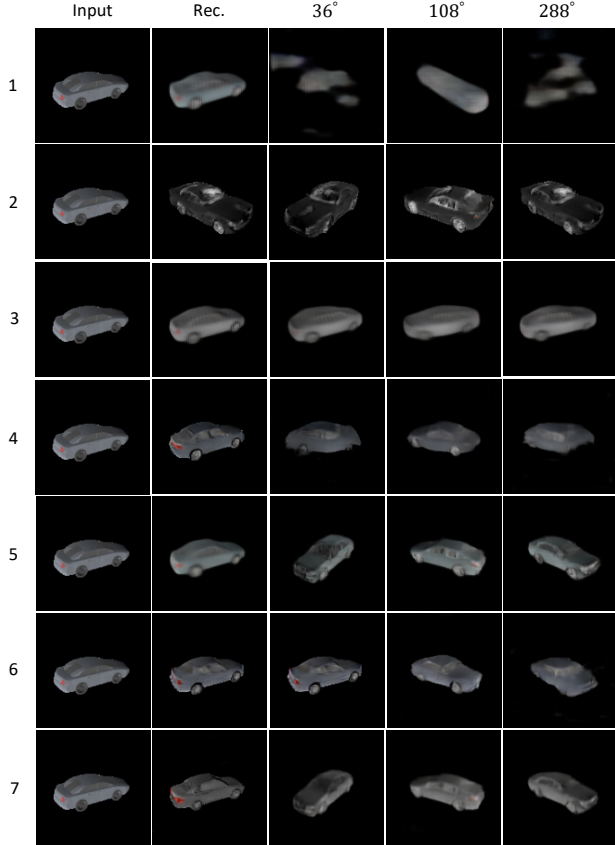


Figure 8. Ablation qualitative results on ShapeNet Cars. The left-most column report experiment ids corresponding to Tab. 5.

Finally, we measured the mean and the standard deviation of the time employed by our finetuning operation (100 steps) over 25 images with two different devices, a NVIDIA GTX 1080 Ti GPU and Intel i7-9700K CPU, achieving a total computation time of $3.817s \pm 0.086$ with the GPU and $42.661s \pm 0.269$ with the CPU.

5.3. Ablation Study

We conduct an ablation study to show the impact of every component of our framework. For these experiments we train our framework on ShapeNet Cars for 50 epochs in Stage 1 and 10 epochs in Stage 2, and we evaluate on the test set using L1 and SSIM (reported into the NVS columns) metrics. We report the quantitative and qualitative NVS results in Tab. 5 and in Fig. 8 respectively. In Fig. 8, from left to right, we show: input, reconstruction using the predicted θ from E , three azimuth rotations of 36° , 108° and 288° respectively. In row 1, we train our framework as an autoencoder with disentangled pose in the latent space and explicit rotations of deep features with a rigid geometric transformation. As shown in the picture, although the reconstruction results are good, we cannot meaningfully rotate the object

due to the lack of explicit multi-view supervision. In row 2 we show the results of the autoencoder after pre-training with Stage 1. Even though the objects can rotate correctly, the car appearance is different and the pose in the reconstruction is wrong. In row 3 we add the Stage 1 pre-training before rebuilding the autoencoder. The model cannot rotate the object, however, each pose generates a realistic car even if with the wrong orientation. We argue that during the second stage the model forgets the good 3D representation learnt during the first stage, supporting our claim. To fight forgetting, we add self-distillation (row 4) and try to reconstruct the generated samples from D_f including also the consistency losses L_z and L_θ . With the former strategy, we can generate novel views of the object, but they are not consistent. Thus, to improve 3D representations, we add the multi-view supervision (row 5) on the generated samples which can be obtained for free. After this addition we are able to rotate the object showing that this is the crucial step for learning 3D features. To further improve the quality of the generated sample, we add an adversarial loss similar to [25] on the real samples (row 6). However, the instability of the adversarial training makes the training prone to collapsing. Finally, with the consistency losses (row 7) L_z and L_θ we can stabilize the adversarial training. From our experiments, the adversarial loss is fundamental in real datasets to achieve sharp results, therefore we kept it on our formulation, even if it does not improve on synthetic datasets.

5.4. Unsupervised Pose Estimation

We report here results regarding the poses inferred by our method from the input image. When evaluating, given the estimated and ground truth poses on the training and validation sets, we first train a linear regressor to map poses from the reference frame implicitly learnt by our model to the ground-truth one of ShapeNet. Then we use it at test time to compare predicted poses to ground truth ones. We note that the scale parameter used in D and the distance to the center of the world ρ used in ShapeNet are inversely linearly related. In terms of metrics, we compute the absolute ρ error (ρ ranging in $[1.0, 1.5]$) and the angle error as the cosine distance between the two azimuths (the angle with 360° range) and report the median for both. Moreover, we calculate the angle prediction accuracy, defined as the ratio of samples with an angle error smaller than 30° with the total number of samples [62].

In the last 3 columns of Tab. 5, we report quantitative pose estimation performance for the Car class of ShapeNet for each combination of the ablation study. The table highlights once more how the key ingredients of our formulation are the self-distillation and multi-view training used in Stage 2. In particular the multi-view training on generated images (row 5), feasible only thanks to our self-distillation, doubles the performance compared to the network after

| | | | | | | | Cars | | | | |
|----|---------|-------------|---------------|------------|-------------|-------------------------|------------------|-----------------|-----------------|---------------------|---------------------|
| | | | | | | | NVS | | Pose Estimation | | |
| Id | Stage 1 | Autoencoder | Self-Distill. | Multi-view | Adversarial | z & θ Consist. | | | | | |
| | | | | | | | $L_1 \downarrow$ | SSIM \uparrow | Acc. \uparrow | Median \downarrow | L1 Rho \downarrow |
| 1 | ✗ | ✓ | ✗ | ✗ | ✗ | ✗ | 15.38 | 0.61 | 6.85 | 91.00 | 0.018 |
| 2 | ✓ | ✗ | ✗ | ✗ | ✗ | ✗ | 13.29 | 0.70 | 36.77 | 40.43 | 0.034 |
| 3 | ✓ | ✓ | ✗ | ✗ | ✗ | ✗ | 13.93 | 0.69 | 36.77 | 40.43 | 0.034 |
| 4 | ✓ | ✓ | ✓ | ✗ | ✗ | ✓ | 12.81 | 0.69 | 16.70 | 88.41 | 0.032 |
| 5 | ✓ | ✓ | ✓ | ✓ | ✗ | ✗ | 7.66 | 0.77 | 86.00 | 5.73 | 0.024 |
| 6 | ✓ | ✓ | ✓ | ✓ | ✓ | ✗ | 14.36 | 0.67 | 14.31 | 92.13 | 0.025 |
| 7 | ✓ | ✓ | ✓ | ✓ | ✓ | ✓ | 7.67 | 0.77 | 86.72 | 5.79 | 0.026 |

Table 5. Ablation study on ShapeNet Cars. For L1 error, pixel values are in $[0, 255]$ range.

Stage 1 (row 2). Moreover, we notice that the network fails when trained without distillation (row 3), failing to generate objects that rotate coherently.

On real datasets we do not estimate the pose error quantitatively due to the lack of GT, therefore we provide a qualitative evaluation in Fig. 9. Given two images I_z and I_θ , we infer the latent representation z from I_z and the pose θ from I_θ . Then, we can generate a new image with the appearance of I_z and the pose of I_θ by simply combining the estimated z and θ . Fig. 9 shows the results of this experiment on the test set of CelebA. We employ the network after finetuning for this experiment. Notably, our method can estimate with high accuracy also challenging poses, such as faces seen from the side, which is an underrepresented pose in the training set.



Figure 9. Qualitative pose estimation on CelebA. We extract θ from I_θ (row 1) and z from I_z (column 1) to craft a novel image.

5.5. Ablation on learned perceptual metrics

In our stage 2 we use multiple losses to measure the similarity between reconstructed images and real ones. Using a very high level subdivision they can be split into losses op-

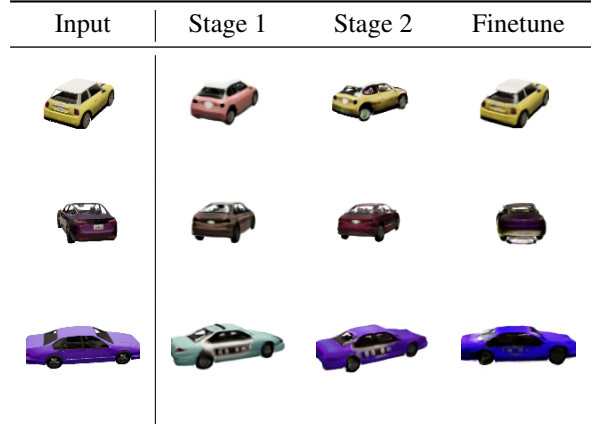


Figure 10. Qualitative comparison of a Stage 1, Stage 2 and finetuning network using as decoder GRAF [53] instead of HoloGAN [40] on the Carla dataset.

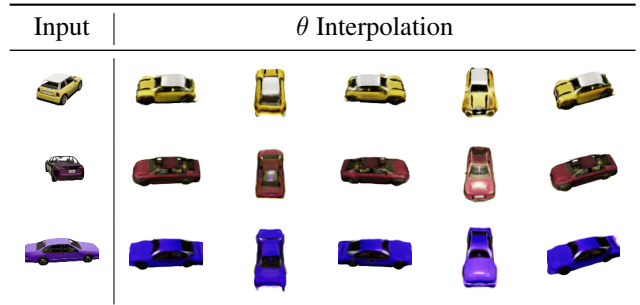


Figure 11. Novel view synthesis from a single input image using as our decoder GRAF [53] instead of HoloGAN [40] on the Carla dataset.

erating directly on pixel intensities (L_2 and L_{SSIM}) and losses operating on a learned deep feature space (L_{VGG} and $Adversarial$). To showcase the impact of the latter for the quality of the generated images we designed an ad-

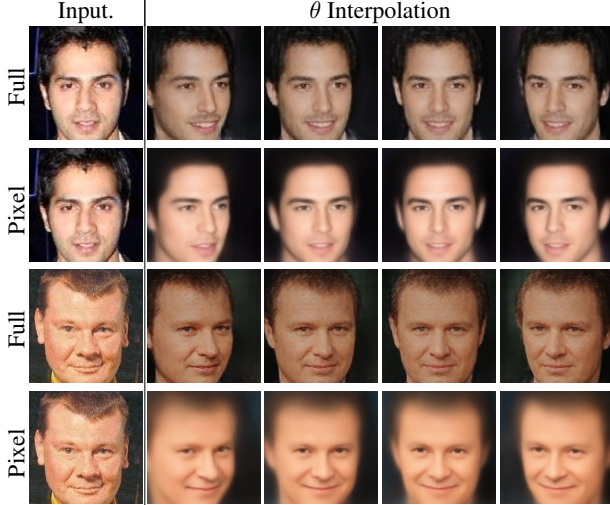


Figure 12. Qualitative comparison between results of Stage 2 with or without losses computed on deep feature spaces.

hoc comparison by training a variant of our model where in stage 2 we optimize only pixel intensities losses (*i.e.*, L_2 and L_{SSIM}). Fig. 12 collects some qualitative results comparing this version of the model to our full formulation. The images generated by the network trained with all losses have two clear advantages with respect to the alternative: they are sharper and contain more details specific of the provided input image (*e.g.* the beard of the man in the top or the hair of the man in the bottom). Both models are able to generate images that resemble the input image.

5.6. Preliminary Results with a Different Decoder

We report preliminary results obtained changing the decoder network in our formulation with the recently proposed neural radiance field based GRAF [53]. While the architecture of the network is quite different from the HoloGAN [40] one used throughout the paper, from a black box perspective, both models allow to provide a latent vector and a pose to generate a view of an object and can therefore be in principle interchanged in our framework.

While the swap does not require major changes, the computational cost of rendering a full image using GRAF is significantly higher. Thus, following the same strategy as its authors, we train on patches. However, the encoder requires an entire image to estimate z and θ . Thus, in stage 1, we initialize GRAF with the pretrained weights released by the authors, and we train only the encoder E to invert images to the generator latent space. Then, in stage 2 due to the patch generation we did not use L_{VGG} and L_{SSIM} to measure the reconstruction error, but we rely only on the pixel-wise L_2 loss. .

In Fig. 10, we report results obtained from a Stage 1, Stage 2 and a Fine-tuned network on the Carla dataset [53]. As we can see from the picture, Stage 1 is not sufficient

to obtain a good reconstruction, while we can recover the identity of the input car in Stage 2. Then, during the fine-tuning we recover some details of the input image such as the color and the pose. In Fig. 11 we report some qualitative results of generated novel views for the same input images showing how the multi-view consistency of the models is maintained.

6. Method Limitations

We notice that sometimes D during Stage 1 fails to converge for some datasets. In such cases, we inherit the same artifacts during Stage 2. For instance, we tried to train on the Bench and on the Chair classes of ShapeNet, however the HoloGAN based D was not able converge, completely collapsing or learning incomplete representations that allow only partial rotations of the objects. In such case, our Stage 2 learns the same incomplete rotations while distilling the generative knowledge. Moreover, we notice that HoloGAN is performing much better on real rather than synthetic datasets. We think that due to the comparatively larger amount of samples in the real datasets the unsupervised learning strategy works better.

7. Conclusions

In this paper we have presented a novel method for NVS from a single view. Our method is the first of its kind that can be trained without requiring any form of annotation or pairing in the training set, the only requirement being a collection of images of objects belonging to the same macro-category. Our method achieves performance comparable to other alternatives on synthetic datasets, while also working on real datasets like CelebA or Cars, where no ground truth is available and the competitors cannot be trained. We tested our framework on NVS with only a single object in the scene. In future, we plan to extend our experiments to scenes containing multiple objects leveraging recently proposed models for scene generation [41, 42].

References

- [1] Martín Abadi, Ashish Agarwal, Paul Barham, Eugene Brevdo, Zhifeng Chen, Craig Citro, Greg S. Corrado, Andy Davis, Jeffrey Dean, Matthieu Devin, Sanjay Ghemawat, Ian Goodfellow, Andrew Harp, Geoffrey Irving, Michael Isard, Yangqing Jia, Rafal Jozefowicz, Lukasz Kaiser, Manjunath Kudlur, Josh Levenberg, Dandelion Mané, Rajat Monga, Sherry Moore, Derek Murray, Chris Olah, Mike Schuster, Jonathon Shlens, Benoit Steiner, Ilya Sutskever, Kunal Talwar, Paul Tucker, Vincent Vanhoucke, Vijay Vasudevan, Fernanda Viégas, Oriol Vinyals, Pete Warden, Martin Wattenberg, Martin Wicke, Yuan Yu, and Xiaoqiang Zheng. TensorFlow: Large-scale machine learning on heterogeneous systems, 2015. Software available from tensorflow.org.

- [2] Rameen Abdal, Yipeng Qin, and Peter Wonka. Image2stylegan: How to embed images into the stylegan latent space? In *Proceedings of the IEEE/CVF International Conference on Computer Vision (ICCV)*, October 2019.
- [3] Rameen Abdal, Yipeng Qin, and Peter Wonka. Image2stylegan++: How to edit the embedded images? In *Proceedings of the IEEE/CVF Conference on Computer Vision and Pattern Recognition (CVPR)*, June 2020.
- [4] Hassan Abu Alhaija, Siva Karthik Mustikovela, Andreas Geiger, and Carsten Rother. Geometric image synthesis. In *Computer Vision – ACCV 2018*, pages 85–100. Springer International Publishing, 2019.
- [5] Brandon Amos, Bartosz Ludwiczuk, and Mahadev Satyanarayanan. Openface: A general-purpose face recognition library with mobile applications. Technical report, CMU-CS-16-118, CMU School of Computer Science, 2016.
- [6] Martin Arjovsky, Soumith Chintala, and Léon Bottou. Wasserstein generative adversarial networks. In *Proceedings of the 34th International Conference on Machine Learning - Volume 70, ICML’17*, page 214–223. JMLR.org, 2017.
- [7] Andrew Brock, Jeff Donahue, and Karen Simonyan. Large scale GAN training for high fidelity natural image synthesis. In *International Conference on Learning Representations*, 2019.
- [8] Angel X. Chang, Thomas Funkhouser, Leonidas Guibas, Pat Hanrahan, Qixing Huang, Zimo Li, Silvio Savarese, Manolis Savva, Shuran Song, Hao Su, Jianxiong Xiao, Li Yi, and Fisher Yu. ShapeNet: An Information-Rich 3D Model Repository. Technical Report arXiv:1512.03012 [cs.GR], Stanford University — Princeton University — Toyota Technological Institute at Chicago, 2015.
- [9] Xu Chen, Jie Song, and Otmar Hilliges. Monocular neural image based rendering with continuous view control. In *Proceedings of the IEEE International Conference on Computer Vision*, pages 4090–4100, 2019.
- [10] Christopher B Choy, Danfei Xu, JunYoung Gwak, Kevin Chen, and Silvio Savarese. 3d-r2n2: A unified approach for single and multi-view 3d object reconstruction. In *Proceedings of the European Conference on Computer Vision (ECCV)*, 2016.
- [11] A. Creswell and A. A. Bharath. Inverting the generator of a generative adversarial network. *IEEE Transactions on Neural Networks and Learning Systems*, 30(7):1967–1974, 2019.
- [12] Paul E Debevec, Camillo J Taylor, and Jitendra Malik. Modeling and rendering architecture from photographs: A hybrid geometry-and image-based approach. In *Proceedings of the 23rd annual conference on Computer graphics and interactive techniques*, pages 11–20, 1996.
- [13] J. Deng, W. Dong, R. Socher, L. Li, Kai Li, and Li Fei-Fei. Imagenet: A large-scale hierarchical image database. In *2009 IEEE Conference on Computer Vision and Pattern Recognition*, pages 248–255, 2009.
- [14] Alexey Dosovitskiy, Jost Tobias Springenberg, and Thomas Brox. Learning to generate chairs with convolutional neural networks. In *Proceedings of the IEEE Conference on Computer Vision and Pattern Recognition*, pages 1538–1546, 2015.
- [15] Emilien Dupont, Miguel Bautista Martin, Alex Colburn, Aditya Sankar, Josh Susskind, and Qi Shan. Equivariant neural rendering. In *International Conference on Machine Learning*, pages 2761–2770. PMLR, 2020.
- [16] Andrew Fitzgibbon, Yonatan Wexler, and Andrew Zisserman. Image-based rendering using image-based priors. *International Journal of Computer Vision*, 63(2):141–151, 2005.
- [17] John Flynn, Michael Broxton, Paul Debevec, Matthew Duvall, Graham Fyffe, Ryan Overbeck, Noah Snavely, and Richard Tucker. Deepview: View synthesis with learned gradient descent. In *Proceedings of the IEEE/CVF Conference on Computer Vision and Pattern Recognition (CVPR)*, June 2019.
- [18] John Flynn, Ivan Neulander, James Philbin, and Noah Snavely. Deepstereo: Learning to predict new views from the world’s imagery. In *Proceedings of the IEEE conference on computer vision and pattern recognition*, pages 5515–5524, 2016.
- [19] Ian Goodfellow, Jean Pouget-Abadie, Mehdi Mirza, Bing Xu, David Warde-Farley, Sherjil Ozair, Aaron Courville, and Yoshua Bengio. Generative adversarial nets. In *Advances in neural information processing systems*, pages 2672–2680, 2014.
- [20] Shanyan Guan, Ying Tai, Bingbing Ni, Feida Zhu, Feiyue Huang, and Xiaokang Yang. Collaborative learning for faster stylegan embedding. In *Proceedings of the IEEE Conference on Computer Vision and Pattern Recognition (CVPR)*, 2021.
- [21] Ishaan Gulrajani, Faruk Ahmed, Martin Arjovsky, Vincent Dumoulin, and Aaron C Courville. Improved training of wasserstein gans. In I. Guyon, U. V. Luxburg, S. Bengio, H. Wallach, R. Fergus, S. Vishwanathan, and R. Garnett, editors, *Advances in Neural Information Processing Systems 30*, pages 5767–5777. Curran Associates, Inc., 2017.
- [22] Nicolai Häni, Selim Engin, Jun-Jee Chao, and Volkan Isler. Continuous object representation networks: Novel view synthesis without target view supervision. In *Proc. NeurIPS*, 2020.
- [23] Paul Henderson and Vittorio Ferrari. Learning single-image 3d reconstruction by generative modelling of shape, pose and shading. *International Journal of Computer Vision*, pages 1–20, 2019.
- [24] Philipp Henzler, Niloy J. Mitra, and Tobias Ritschel. Escaping plato’s cave: 3d shape from adversarial rendering. In *The IEEE International Conference on Computer Vision (ICCV)*, October 2019.
- [25] Phillip Isola, Jun-Yan Zhu, Tinghui Zhou, and Alexei A. Efros. Image-to-image translation with conditional adversarial networks. In *Proceedings of the IEEE Conference on Computer Vision and Pattern Recognition (CVPR)*, July 2017.
- [26] Phillip Isola, Jun-Yan Zhu, Tinghui Zhou, and Alexei A. Efros. Image-to-image translation with conditional adversarial networks. In *Proceedings of the IEEE conference on computer vision and pattern recognition*, pages 1125–1134, 2017.
- [27] Dinghuang Ji, Junghyun Kwon, Max McFarland, and Silvio Savarese. Deep view morphing. In *Proceedings of the*

- IEEE Conference on Computer Vision and Pattern Recognition*, pages 2155–2163, 2017.
- [28] Tero Karras, Samuli Laine, and Timo Aila. A style-based generator architecture for generative adversarial networks. In *Proceedings of the IEEE/CVF Conference on Computer Vision and Pattern Recognition (CVPR)*, June 2019.
 - [29] Diederik P. Kingma and Jimmy Ba. Adam: A method for stochastic optimization. In *3rd International Conference on Learning Representations (ICLR)*, 2015.
 - [30] Diederik P. Kingma and Max Welling. Auto-encoding variational bayes. In *2nd International Conference on Learning Representations, ICLR 2014, Banff, AB, Canada, April 14-16, 2014, Conference Track Proceedings*, 2014.
 - [31] Marek Kowalski, Stephan J. Garbin, Virginia Estellers, Tadas Baltrušaitis, Matthew Johnson, and Jamie Shotton. Config: Controllable neural face image generation. In *European Conference on Computer Vision (ECCV)*, 2020.
 - [32] Yiyi Liao, Katja Schwarz, Lars Mescheder, and Andreas Geiger. Towards unsupervised learning of generative models for 3d controllable image synthesis. In *Proceedings of the IEEE/CVF Conference on Computer Vision and Pattern Recognition (CVPR)*, June 2020.
 - [33] Chen-Hsuan Lin, Chen Kong, and Simon Lucey. Learning efficient point cloud generation for dense 3d object reconstruction. In *AAAI*, 2018.
 - [34] Xiaofeng Liu, Tong Che, Yiqun Lu, Chao Yang, Site Li, and Jane You. Auto3d: Novel view synthesis through unsupervisedly learned variational viewpoint and global 3d representation. In *Proceedings of the European Conference on Computer Vision (ECCV)*, 2020.
 - [35] Ziwei Liu, Ping Luo, Xiaogang Wang, and Xiaoou Tang. Deep learning face attributes in the wild. In *Proceedings of International Conference on Computer Vision (ICCV)*, December 2015.
 - [36] Stephen Lombardi, Tomas Simon, Jason Saragih, Gabriel Schwartz, Andreas Lehrmann, and Yaser Sheikh. Neural volumes: learning dynamic renderable volumes from images. *ACM Transactions on Graphics (TOG)*, 38(4):65, 2019.
 - [37] Xudong Mao, Qing Li, Haoran Xie, Raymond Y.K. Lau, Zhen Wang, and Stephen Paul Smolley. Least squares generative adversarial networks. In *Proceedings of the IEEE International Conference on Computer Vision (ICCV)*, Oct 2017.
 - [38] Ben Mildenhall, Pratul P Srinivasan, Matthew Tancik, Jonathan T Barron, Ravi Ramamoorthi, and Ren Ng. Nerf: Representing scenes as neural radiance fields for view synthesis. In *Proceedings of the European Conference on Computer Vision (ECCV)*, 2020.
 - [39] Takeru Miyato, Toshiki Kataoka, Masanori Koyama, and Yuichi Yoshida. Spectral normalization for generative adversarial networks. In *International Conference on Learning Representations*, 2018.
 - [40] Thu Nguyen-Phuoc, Chuan Li, Lucas Theis, Christian Richardt, and Yong-Liang Yang. Hologan: Unsupervised learning of 3d representations from natural images. In *Proceedings of the IEEE/CVF International Conference on Computer Vision (ICCV)*, October 2019.
 - [41] Thu Nguyen-Phuoc, Christian Richardt, Long Mai, Yong-Liang Yang, and Niloy Mitra. Blockgan: Learning 3d object-aware scene representations from unlabelled images. *arXiv*, 2020.
 - [42] Michael Niemeyer and Andreas Geiger. Giraffe: Representing scenes as compositional generative neural feature fields, 2021.
 - [43] Michael Niemeyer, Lars Mescheder, Michael Oechsle, and Andreas Geiger. Differentiable volumetric rendering: Learning implicit 3d representations without 3d supervision. In *Proceedings of the IEEE/CVF Conference on Computer Vision and Pattern Recognition (CVPR)*, June 2020.
 - [44] Augustus Odena, Vincent Dumoulin, and Chris Olah. Deconvolution and checkerboard artifacts. *Distill*, 2016.
 - [45] Michael Oechsle, Lars Mescheder, Michael Niemeyer, Thilo Strauss, and Andreas Geiger. Texture fields: Learning texture representations in function space. In *Proceedings of the IEEE/CVF International Conference on Computer Vision (ICCV)*, October 2019.
 - [46] Kyle Olszewski, Sergey Tulyakov, Oliver Woodford, Hao Li, and Linjie Luo. Transformable bottleneck networks. In *Proceedings of the IEEE International Conference on Computer Vision*, pages 7648–7657, 2019.
 - [47] Eunbyung Park, Jimei Yang, Ersin Yumer, Duygu Ceylan, and Alexander C Berg. Transformation-grounded image generation network for novel 3d view synthesis. In *Proceedings of the IEEE conference on computer vision and pattern recognition*, pages 3500–3509, 2017.
 - [48] Taesung Park, Ming-Yu Liu, Ting-Chun Wang, and Jun-Yan Zhu. Semantic image synthesis with spatially-adaptive normalization. In *Proceedings of the IEEE/CVF Conference on Computer Vision and Pattern Recognition (CVPR)*, June 2019.
 - [49] Jhony K Pontes, Chen Kong, Sridha Sridharan, Simon Lucey, Anders Eriksson, and Clinton Fookes. Image2mesh: A learning framework for single image 3d reconstruction. In *Asian Conference on Computer Vision*, pages 365–381. Springer, 2018.
 - [50] Alec Radford, Luke Metz, and Soumith Chintala. Unsupervised representation learning with deep convolutional generative adversarial networks. In *International Conference on Learning Representations (ICLR)*, 2016.
 - [51] Konstantinos Rematas, Ricardo Martin-Brualla, and Vittorio Ferrari. Sharf: Shape-conditioned radiance fields from a single view. In *ICML*, 2021.
 - [52] Helge Rhodin, Mathieu Salzmann, and Pascal Fua. Unsupervised geometry-aware representation for 3d human pose estimation. In *Proceedings of the European Conference on Computer Vision (ECCV)*, September 2018.
 - [53] Katja Schwarz, Yiyi Liao, Michael Niemeyer, and Andreas Geiger. Graf: Generative radiance fields for 3d-aware image synthesis. In *European Conference on Computer Vision (ECCV)*, 2020.
 - [54] Steven M Seitz, Brian Curless, James Diebel, Daniel Scharstein, and Richard Szeliski. A comparison and evaluation of multi-view stereo reconstruction algorithms. In *2006 IEEE computer society conference on computer vision and*

- pattern recognition (CVPR'06)*, volume 1, pages 519–528. IEEE, 2006.
- [55] Karen Simonyan and Andrew Zisserman. Very deep convolutional networks for large-scale image recognition. In *International Conference on Learning Representations*, 2015.
 - [56] Vincent Sitzmann, Justus Thies, Felix Heide, Matthias Nießner, Gordon Wetzstein, and Michael Zollhofer. Deepvoxels: Learning persistent 3d feature embeddings. In *Proceedings of the IEEE Conference on Computer Vision and Pattern Recognition*, pages 2437–2446, 2019.
 - [57] Vincent Sitzmann, Michael Zollhöfer, and Gordon Wetzstein. Scene representation networks: Continuous 3d-structure-aware neural scene representations. In *Advances in Neural Information Processing Systems*, pages 1121–1132, 2019.
 - [58] Shao-Hua Sun, Minyoung Huh, Yuan-Hong Liao, Ning Zhang, and Joseph J Lim. Multi-view to novel view: Synthesizing novel views with self-learned confidence. In *Proceedings of the European Conference on Computer Vision (ECCV)*, pages 155–171, 2018.
 - [59] Maxim Tatarchenko, Alexey Dosovitskiy, and Thomas Brox. Multi-view 3d models from single images with a convolutional network. In *European Conference on Computer Vision*, pages 322–337. Springer, 2016.
 - [60] Yu Tian, Xi Peng, Long Zhao, Shaoting Zhang, and Dimitris N Metaxas. Cr-gan: learning complete representations for multi-view generation. *arXiv*, 2018.
 - [61] Luan Tran, Xi Yin, and Xiaoming Liu. Disentangled representation learning gan for pose-invariant face recognition. In *Proceedings of the IEEE conference on computer vision and pattern recognition*, pages 1415–1424, 2017.
 - [62] Shubham Tulsiani, Alexei A. Efros, and Jitendra Malik. Multi-view consistency as supervisory signal for learning shape and pose prediction. In *Proceedings of the IEEE Conference on Computer Vision and Pattern Recognition (CVPR)*, June 2018.
 - [63] Xiaolong Wang and Abhinav Gupta. Generative image modeling using style and structure adversarial networks. In *Computer Vision – ECCV 2016*. Springer International Publishing, 2016.
 - [64] Zhou Wang, Alan C Bovik, Hamid R Sheikh, and Eero P Simoncelli. Image quality assessment: from error visibility to structural similarity. *IEEE transactions on image processing*, 13(4):600–612, 2004.
 - [65] Daniel E Worrall, Stephan J Garbin, Daniyar Turmukhambetov, and Gabriel J Brostow. Interpretable transformations with encoder-decoder networks. In *Proceedings of the IEEE International Conference on Computer Vision*, pages 5726–5735, 2017.
 - [66] Shangzhe Wu, Christian Rupprecht, and Andrea Vedaldi. Unsupervised learning of probably symmetric deformable 3d objects from images in the wild. In *Proceedings of the IEEE/CVF Conference on Computer Vision and Pattern Recognition*, pages 1–10, 2020.
 - [67] Zongze Wu, Dani Lischinski, and Eli Shechtman. Stylespace analysis: Disentangled controls for stylegan image generation. In *Proceedings of the IEEE Conference on Computer Vision and Pattern Recognition (CVPR)*, 2021.
 - [68] Junyuan Xie, Ross Girshick, and Ali Farhadi. Deep3d: Fully automatic 2d-to-3d video conversion with deep convolutional neural networks. In *European Conference on Computer Vision*, pages 842–857. Springer, 2016.
 - [69] Xiaogang Xu, Ying-Cong Chen, and Jiaya Jia. View independent generative adversarial network for novel view synthesis. In *Proceedings of the IEEE International Conference on Computer Vision*, pages 7791–7800, 2019.
 - [70] Yinghao Xu, Yujun Shen, Jiapeng Zhu, Ceyuan Yang, and Bolei Zhou. Generative hierarchical features from synthesizing images, 2021.
 - [71] Jimei Yang, Scott E Reed, Ming-Hsuan Yang, and Honglak Lee. Weakly-supervised disentangling with recurrent transformations for 3d view synthesis. In *Advances in Neural Information Processing Systems*, pages 1099–1107, 2015.
 - [72] Linjie Yang, Ping Luo, Chen Change Loy, and Xiaoou Tang. A large-scale car dataset for fine-grained categorization and verification. In *Proceedings of the IEEE conference on computer vision and pattern recognition*, pages 3973–3981, 2015.
 - [73] Mingyu Yin, Li Sun, and Qingli Li. Novel view synthesis on unpaired data by conditional deformable variational auto-encoder. In *Proceedings of the European Conference on Computer Vision (ECCV)*, 2020.
 - [74] Alex Yu, Vickie Ye, Matthew Tancik, and Angjoo Kanazawa. pixelnerf: Neural radiance fields from one or few images. In *Proceedings of the IEEE/CVF Conference on Computer Vision and Pattern Recognition (CVPR)*, pages 4578–4587, June 2021.
 - [75] Tinghui Zhou, Shubham Tulsiani, Weilun Sun, Jitendra Malik, and Alexei A Efros. View synthesis by appearance flow. In *European Conference on Computer Vision*, 2016.
 - [76] Jun-Yan Zhu, Philipp Krähenbühl, Eli Shechtman, and Alexei A. Efros. Generative visual manipulation on the natural image manifold. In *Computer Vision – ECCV 2016*. Springer International Publishing, 2016.
 - [77] Jun-Yan Zhu, Zhoutong Zhang, Chengkai Zhang, Jiajun Wu, Antonio Torralba, Josh Tenenbaum, and Bill Freeman. Visual object networks: Image generation with disentangled 3d representations. In S. Bengio, H. Wallach, H. Larochelle, K. Grauman, N. Cesa-Bianchi, and R. Garnett, editors, *Advances in Neural Information Processing Systems 31*, pages 118–129. Curran Associates, Inc., 2018.
 - [78] Xiangyu Zhu, Zhen Lei, Xiaoming Liu, Hailin Shi, and Stan Z Li. Face alignment across large poses: A 3d solution. In *Proceedings of the IEEE conference on computer vision and pattern recognition*, pages 146–155, 2016.
 - [79] Zhenyao Zhu, Ping Luo, Xiaogang Wang, and Xiaoou Tang. Multi-view perceptron: a deep model for learning face identity and view representations. In *Advances in Neural Information Processing Systems*, pages 217–225, 2014.